Supporting Information for

Relationship between the tropical tropopause and tropical easterly jet streams over Indian monsoon region

Sanjay K. Mehta*, †, Vanmathi A, Saleem Ali, Aravindhavel A, and Ramesh Reddy
SRM Research Institute, SRM Institute of Science and Technology, Kattankulathur, 603203, India

*Corresponding author: Sanjay Mehta (ksanjaym@gmail.com)

†This work was partially carried out when author was at National Atmospheric Research Laboratory (NARL), Gadanki, 517502, India

Contents of this file

This supporting material contains

Figures S1 to S13

Tables ST1 to ST2

Instructions to download radiosonde data from NARL webpage (Page 1 to 3)

Introduction

This supporting information provides the additional figures and tables and their description to support the main article.

Adiabatic and Diabatic Processes

As there is no heat input in the adiabatic process, an increase in height of the parcel will lead to a decrease in its temperature and vice versa i.e. height and temperature are out of phase. However, in the diabatic process, heat is added (diabatic heating) or removed (diabatic cooling) to system from the surrounding will increase or decrease the temperature of the parcel (Wallace & Hobbs, 2006).

Similarity between Zonal Wind and Temperature

To examine the similarity of zonal wind temperature, we have obtained the correlation between them over the altitude of ~12-22 km (Supplementary Fig. S1). It is found that 27% profiles are strongly correlated (r> 0.7) and 55% of the profiles are moderately correlated (0.3<r<0.7) while remaining 15% profiles shows no dependence and 3% profiles are anti-correlated. That is ~ 82% profiles more or less show a similarity between temperature and zonal wind. We have also checked the sensitivity of the correlation on the choice of the altitude and obtained the correlation between temperature and zonal wind over 14-20 km which does not show any major difference. Such similarity between temperature and zonal wind indicates the possibility of a relationship between TEJ and CPT.

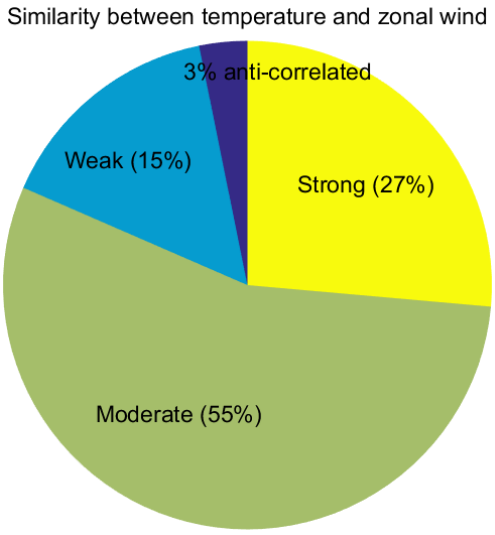

Figure S1*. The percentage of the occurrence strong (r>0.7), moderate (0.3<r<0.7) and weak (r<0.3) correlation between temperature and zonal wind profiles from the altitude of ~12-22 km over the period JJA 2006-2014.*

Thermal wind balance

To illustrate the thermal wind balance due to TEJ streams we have obtained the temperature profiles from the India Meteorological Department (IMD) station, Chennai (13.0°N, 80.04°E) which is meridionally separated by about half a degree from Gadanki. The IMD radiosonde data for Chennai (Madras) station code (43279 or VOMM) is available from the link http://weather.uwyo.edu/upperair/sounding.html. However, as the radiosonde observations over Chennai simultaneous to Gadanki observations on the typical dates mentioned in Figure 1 (main article) were not available. Thus, we have taken another set of similar typical examples as shown in Figure S2. For the sharp case, H_{CPT} and H_{TEJ} occur at the same altitude ~ 16.6 km as observed on 10 July 2013. A strong TEJ stream with peak speed ~53 m/s located exactly in the vicinity of the tropopause (T_{CPT} ~190 K) is observed. We have calculated the meridional temperature gradient between Chennai (13.0 N) and Gadanki (13.48 N) and then obtained the right-hand side term of equation 1 (hereafter referred as meridional temperature gradient ($\frac{\partial T}{\partial y}$) term). It is observed that the zonal wind shear ($\frac{\partial U}{\partial z}$) and $\frac{\partial T}{\partial y}$ term between the altitudes 15.1 -17.7 km are roughly the same indicating that the TEJ is in the thermal wind balance in the above-mentioned layer. Similarly, the case observed on 18 August 2010 when TEJ has broad (15.9-16.9 km) peak, the tropopause is also observed to be relatively broader. The presence of the temperature inversions at 15.9 km and 16.9 km on the lower and upper edges of the TEJ broad peak can also be noticed. In this case, $\frac{\partial U}{\partial z}$ and $\frac{\partial T}{\partial y}$ term show a good similarity between 14.4 -17.4 km indicating that TEJ is in thermal wind balance. In the case of the multiple TEJ peaks observed at 16 km (speed ~39.4 m/s) and 18 km (speed ~ 34 m/s) are associated with multiple tropopauses occurring at the same altitudes 16 km (temperature ~193.2 K) and 18 km (T_{CPT}~191 K) respectively. In this case peak of the TEJ (H_{TEJ}) lies ~ 2 km below the H_{CPT} coinciding with temperature inversion present in the UT (Fujiwara et al. 2003) which is in thermal wind balance.

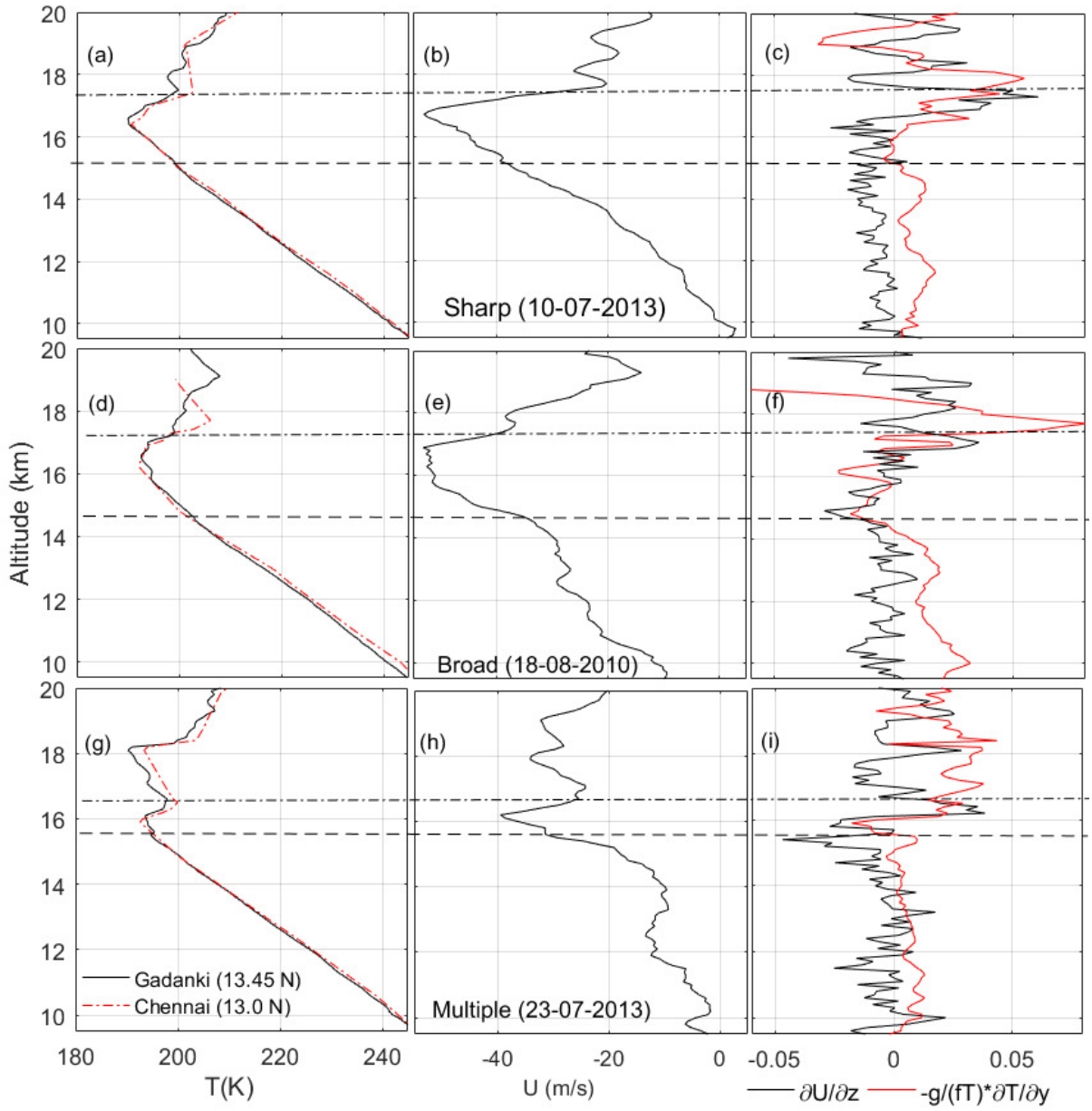

Figure S2. *Typical profiles of (a) temperature, (b) zonal wind and (c) zonal wind shear (left-hand side of equation 1) and the term involving meridional temperature gradient (right-hand side of equation 1) for sharp tropopause and TEJ observed on 10 July 2013. (d – f) and (g-i) are the same as Figures 1a-c but for broad tropopause and TEJ and multiple tropopauses and TEJ observed on 23 July 2013, respectively. Dashed and dash-dotted lines represent the altitudes between which TEJ is in the thermal wind balance.*

Temporal variation of H_{CPT} and H_{TEJ} and an approach to quantify its relationship

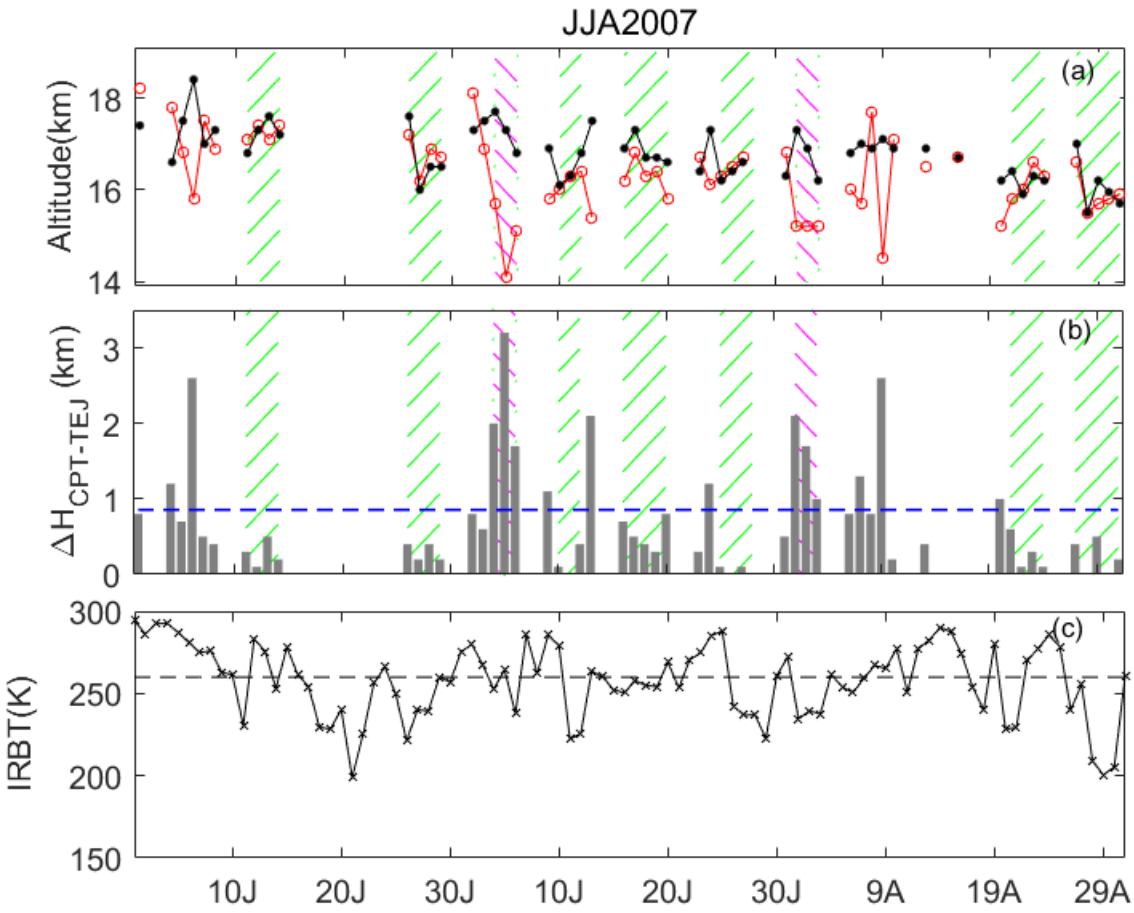

Figure S3(a) Day to day variability of H_{CPT} and H_{TEJ}during the Indian summer monsoon seasons 2006. (b) Time series of ΔH (the difference between H_{CPT} and H_{TEJ}) along with mean ΔH over the period. (c) day to day variation of the infrared brightness temperature (IRBT).

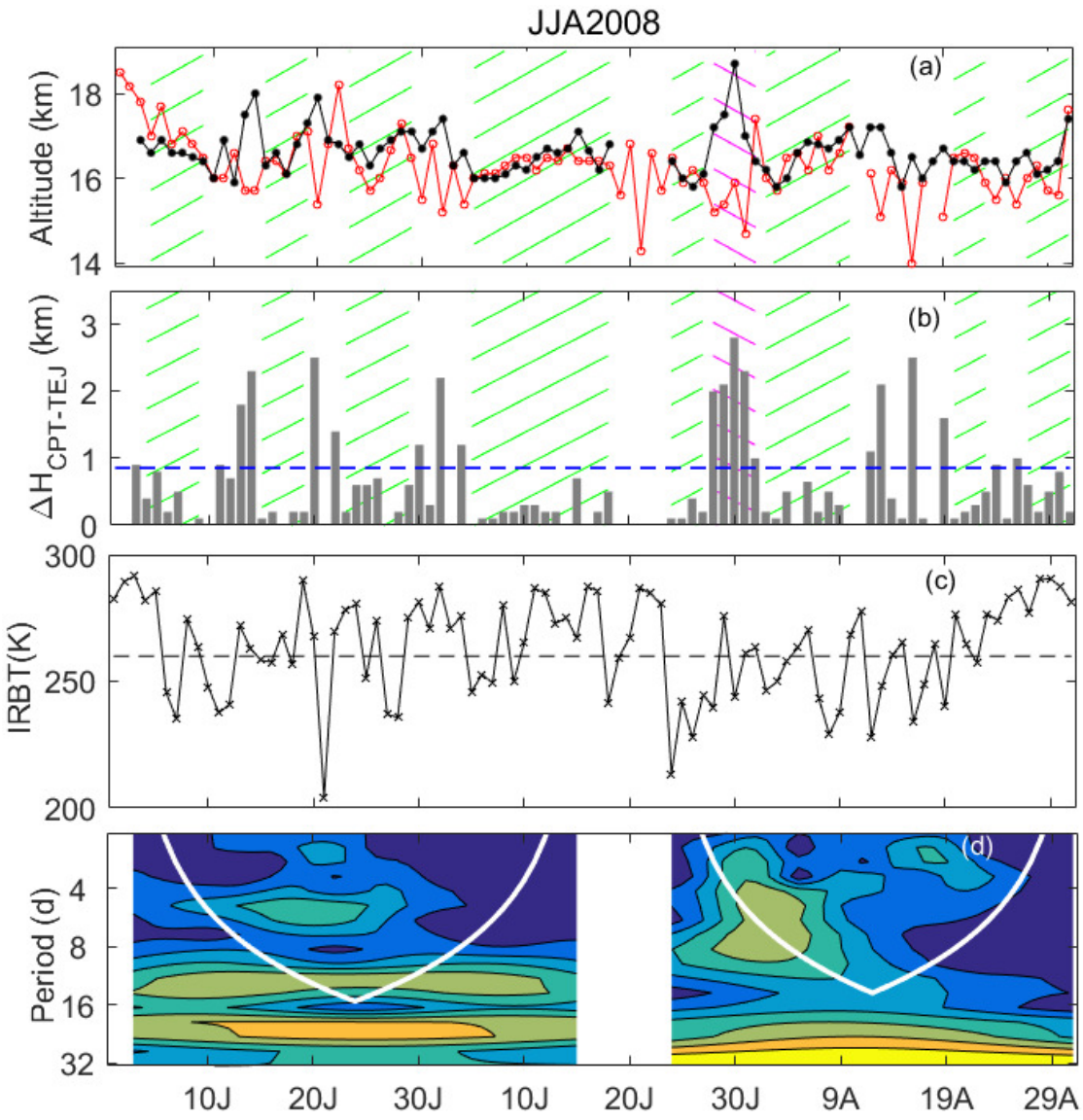

Figure S4 (a) Day to day variability of H_{CPT} and H_{TEJ} during the Indian summer monsoon seasons 2006. (b) Time series of ΔH (the difference between H_{CPT} and H_{TEJ}) along with mean ΔH over the period. (c) day to day variation of the Infrared brightness temperature (IRBT) and (d) Wavelet spectrum of temperature (in terms of power) at 16 km altitude. White curve represents cone of influence.

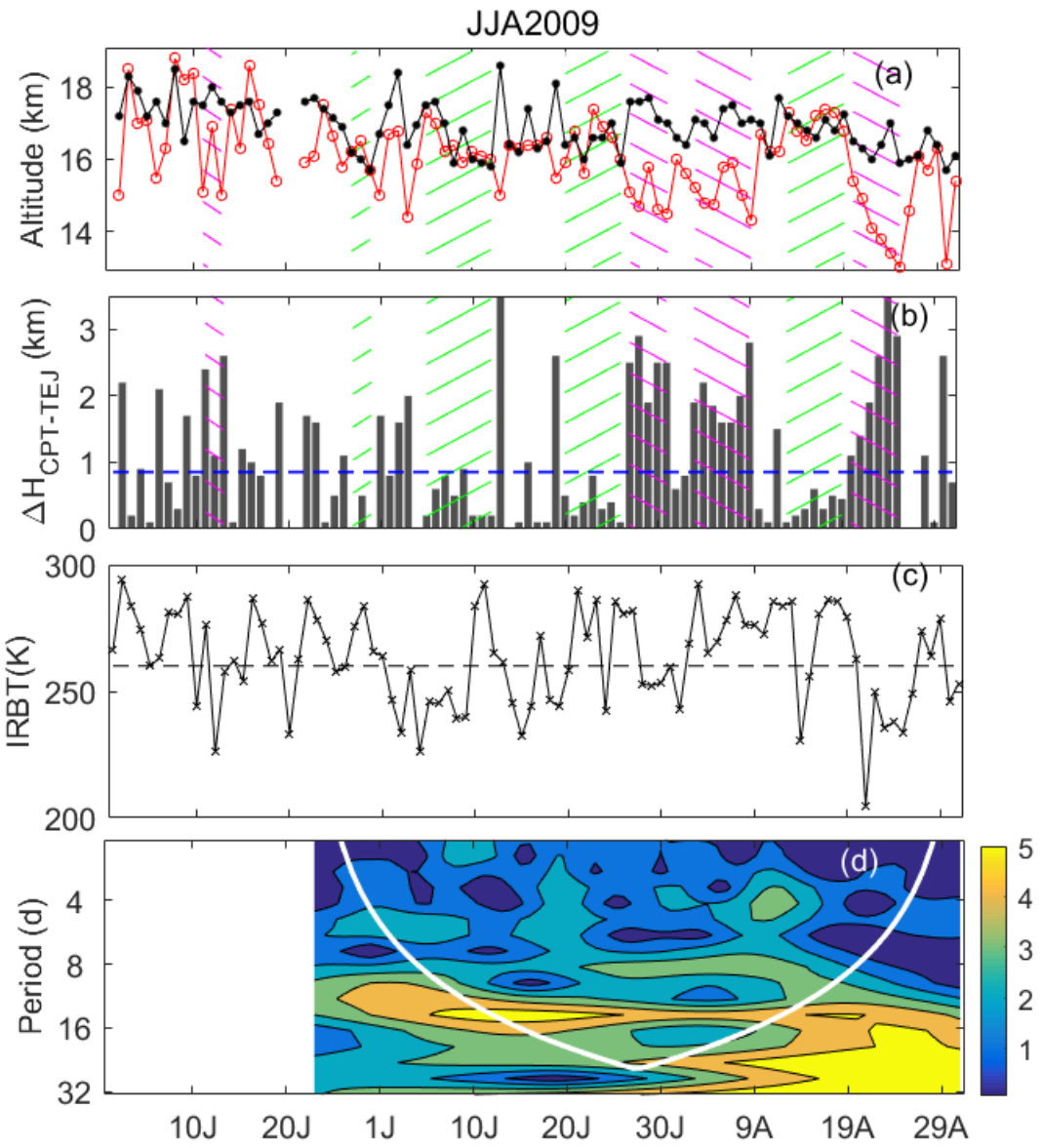

Figure S5. (a)-(d) are same as Figure S4 (a)-(d) but observed during JJA 2009.

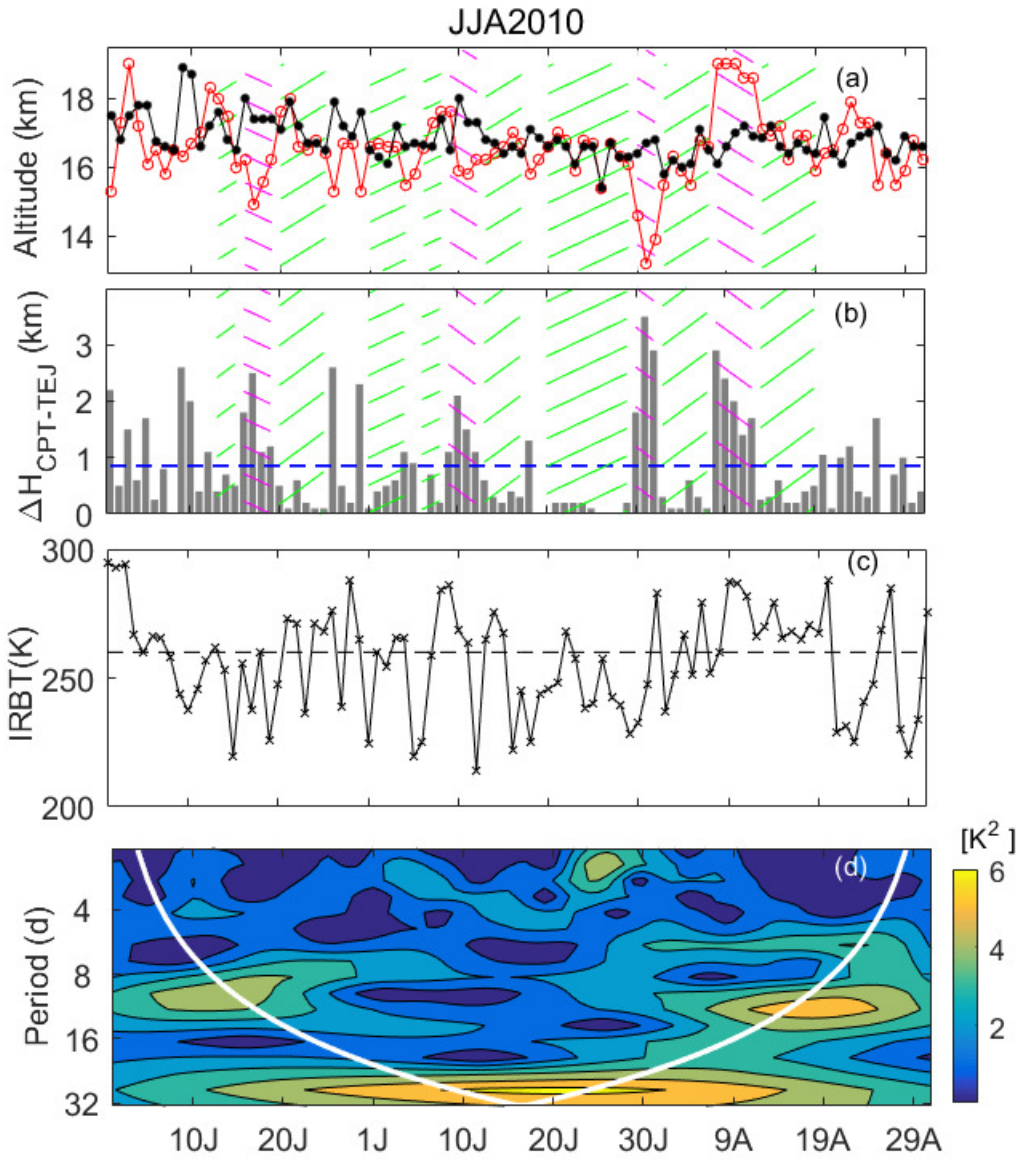

Figure S6. (a)-(d) are same as Figure S4 (a)-(d) but observed during JJA 2010.

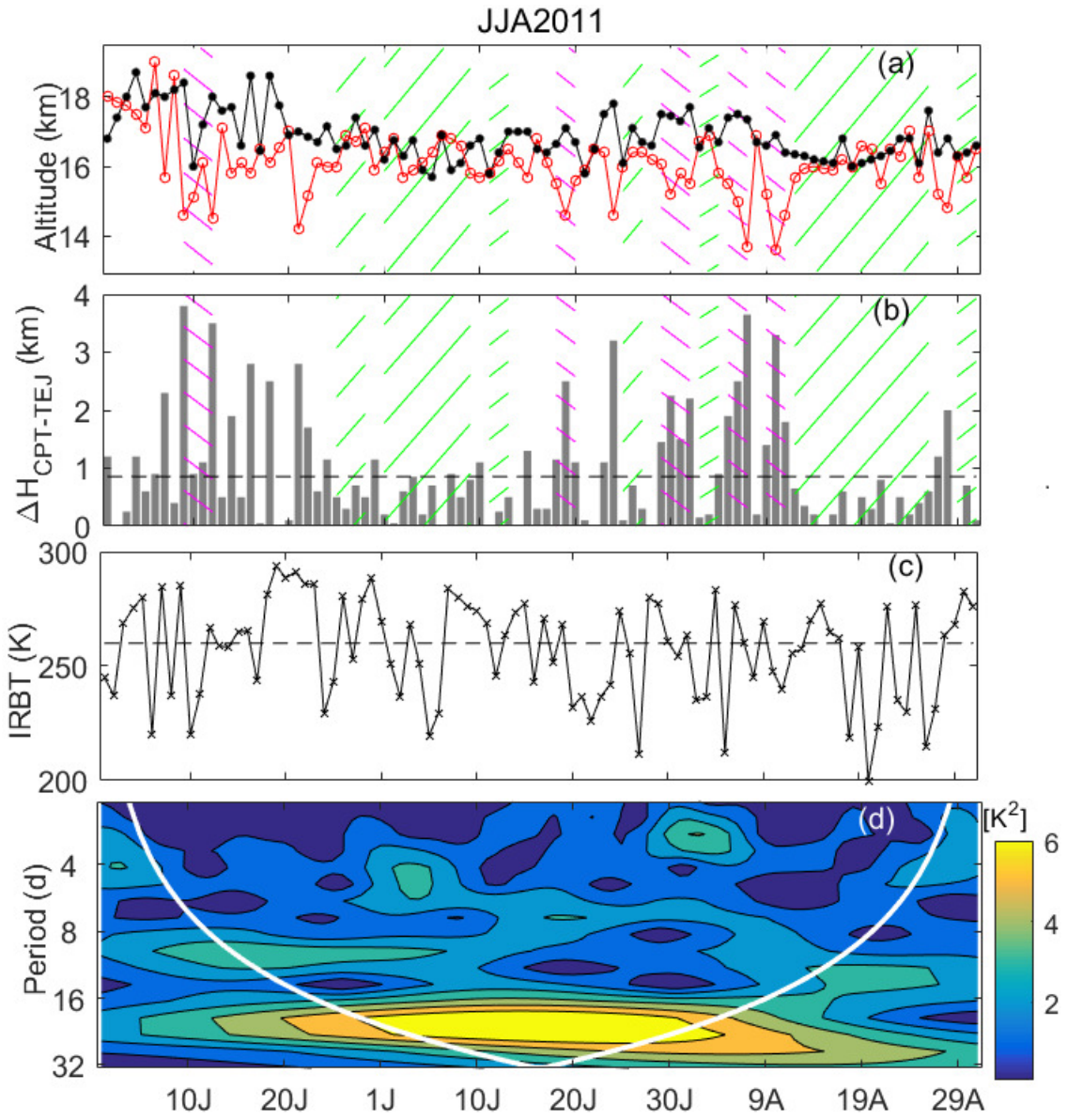

Figure S7. (a)-(d) are same as Figure S4 (a)-(d) but observed during JJA 2011.

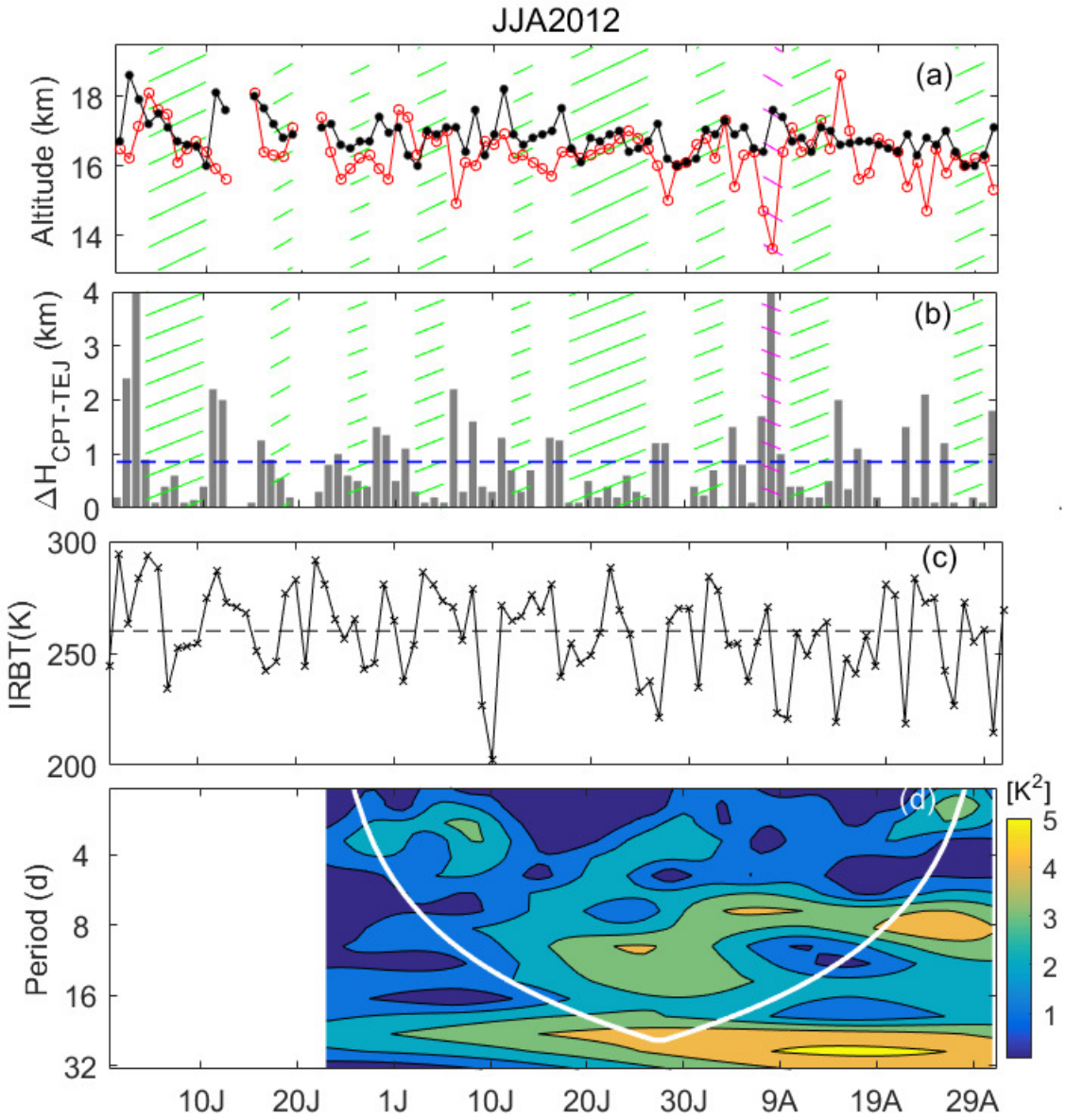

Figure S8. (a)-(d) are same as Figure S4 (a)-(d) but observed during JJA 2012.

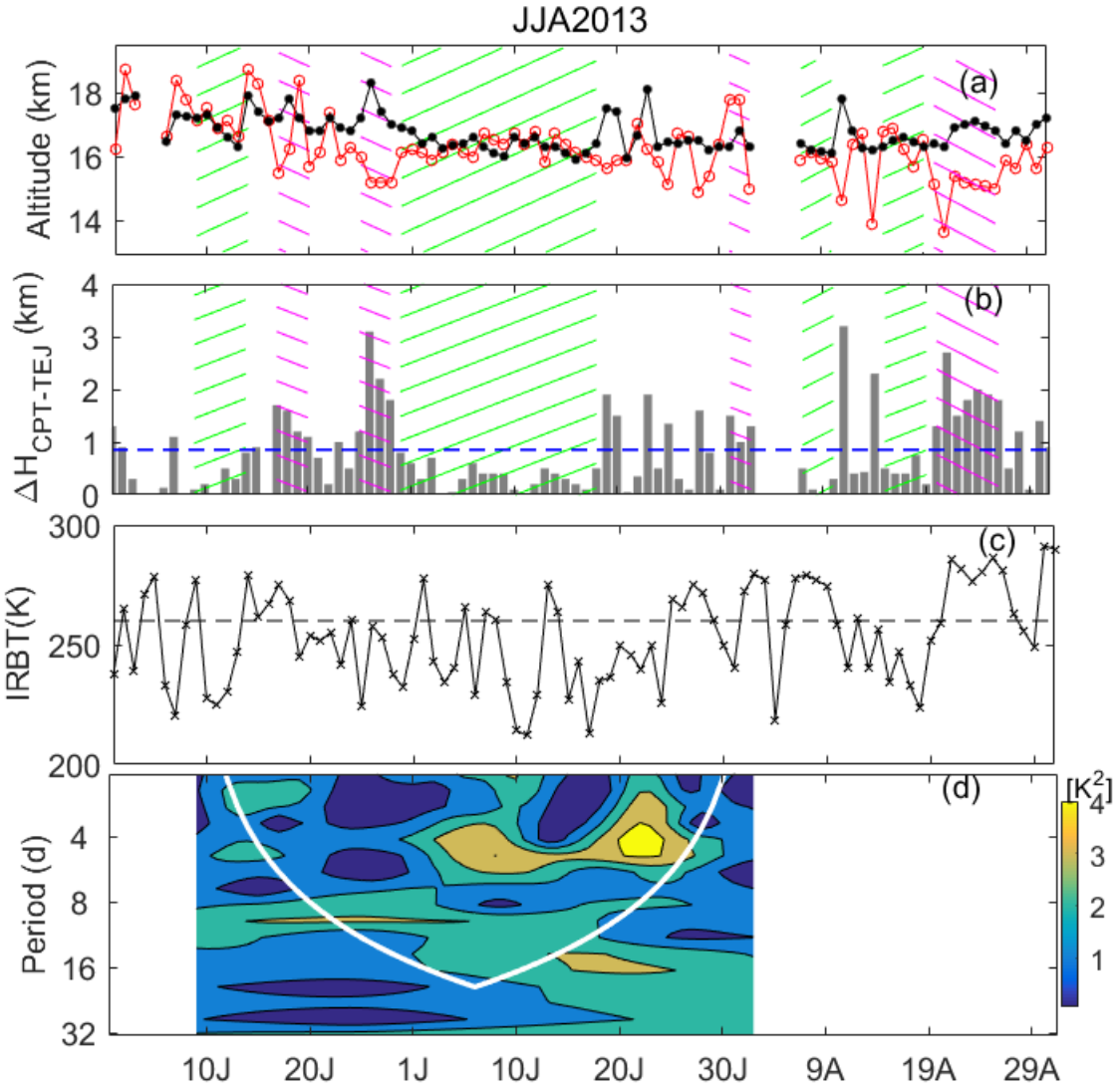

Figure S9. (a)-(d) are same as Figure S4 (a)-(d) but observed during JJA 2013.

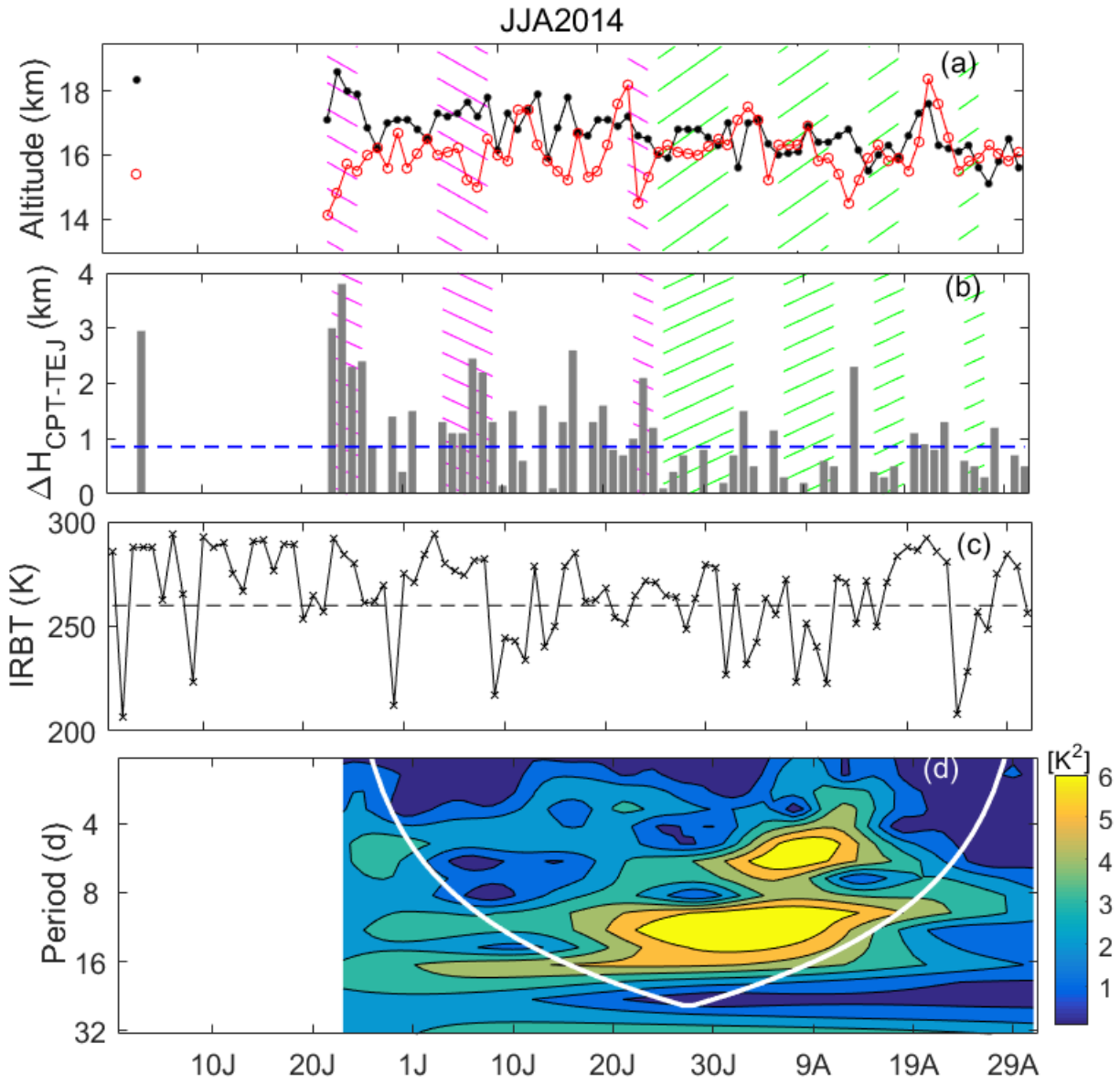

Figure S10. (a)-(d) are same as Figure S4 (a)-(d) but observed during JJA 2014.

Probability of distribution of day-to-day difference of H_{CPT} and H_{TEJ} and $\overline{\Delta H}_{CPT-TEJ}$

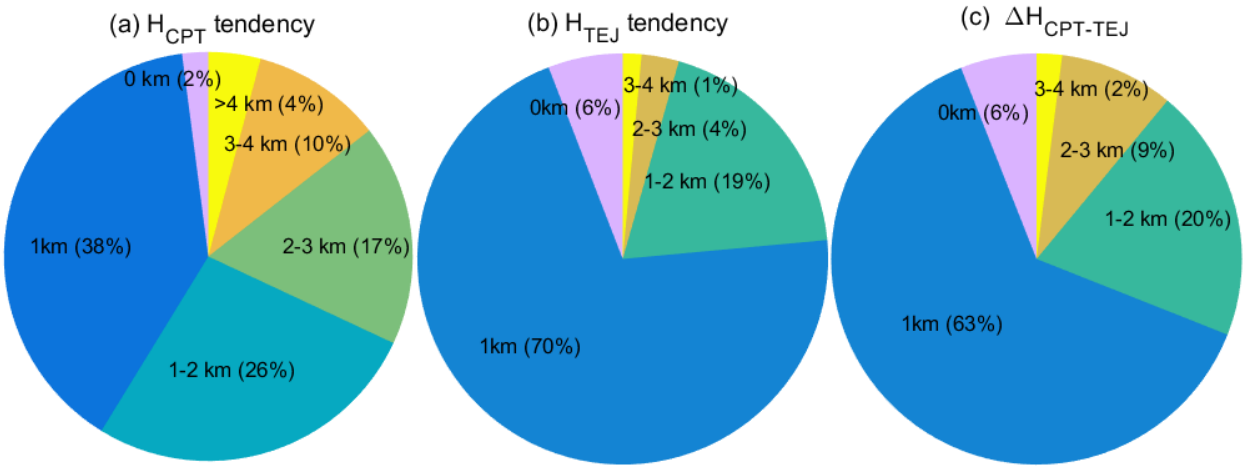

Figure S11. (a)The percentage of the occurrence of the absolute change of the H_{CPT} tendency within 1 km, 1-2 km, 2-3 km, 3-4 km and >4 km calculated over the period JJA 2006-2014. (b) ate (c) are the same as (a) but for the H_{TEJ} tendency and $\Delta H_{CPT-TEJ}$, respectively.

Role of the convection on the relationship between H_{CPT} and H_{TEJ}

We have investigated the roles of the convection occurring at different heights (convection top height; CTH) on the relationship H_{CPT} and H_{TEJ} using threshold criteria following Meenu et al., (2010). We have obtained the IRBT probability distribution for category1 (category2) which shows that about 4% (5%), 13% (8%), 10% (13%), 42% (36%), 16% (18%) and 15% (20%) data falls under <220K, 220-235K, 235-245K, 245-270K, 270-280K and >280K, representing the CTH >12 km, 10-12km, 8-10 km, 5-8 km, 2-5 km and no convection, respectively. It is observed occurrence of the category1 and category2 does not depend upon the local convection.

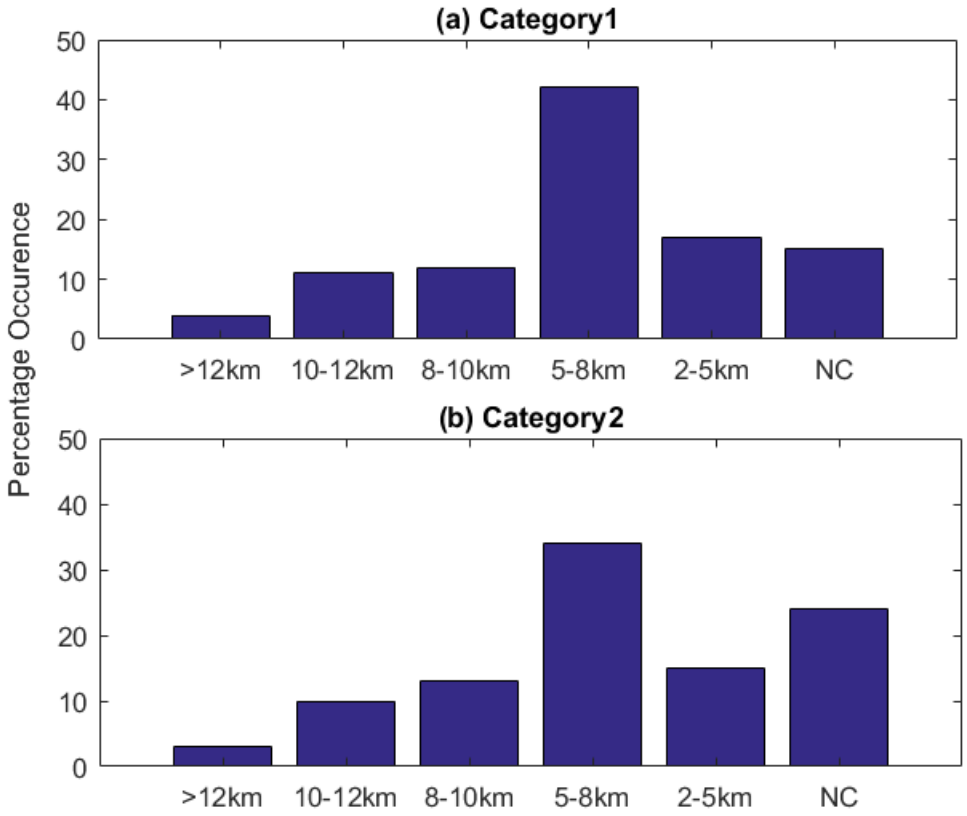

***Figure S12**. Probability distributions of the (a) category1 and (b)category2*

Relationship between CPT, LRT and TEJ

During ISM season deep convections occur frequently and it is known that H_{CPT} and altitude of the lapse rate tropopause (LRT) (H_{LRT}) may coincide at the same altitude (Seidel et al., 2001). Note that LRT is defined based on the lapse rate criteria (Highwood & Hoskins, 1998). To understand the relationship between H_{CPT} , H_{LRT} and H_{TEJ}, their day to day variations are shown in Supplementary Figure S11. We found that LRT coincides to the CPT ~26% times under category1 while 15% times under category2. Out of these coincident cases, the majority (89% under category1 and 85% under category2) occurs during convection however not necessarily with deep convection always. TEJ lies in between CPT and LRT ~24% and 7% times under category 1 and category 2, respectively. Note that TEJ frequently (77% times) occur above the LRT under category1 while it frequently (74% times) occur below the LRT under category2. However, as LRT has limited physical relevance, we have focused on the relationship between CPT and TEJ only.

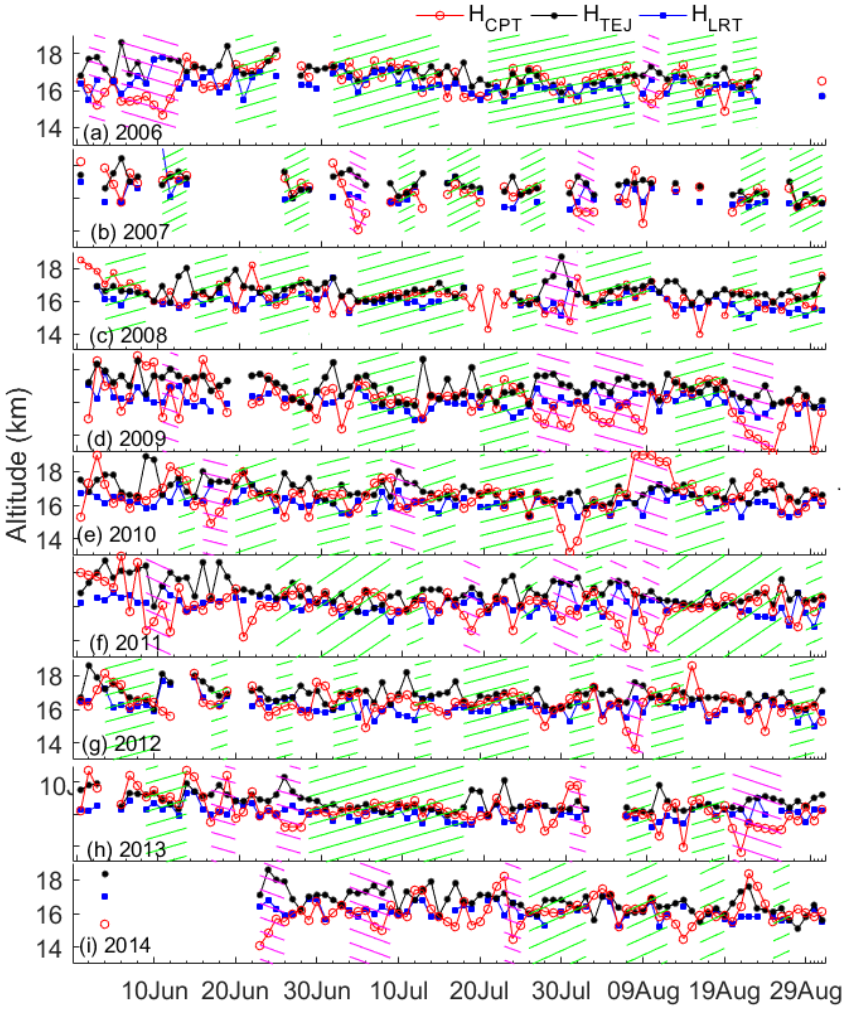

Figure S13. Day to day variability of H_{CPT}, H_{LRT} and H_{TEJ} during the Indian summer monsoon seasons (2006-2014).

Correlation analysis

Table ST1 lists the correlation coefficients between H_{CPT} and H_{TEJ}, T_{CPT} and H_{TEJ}, H_{CPT} and T_{CPT} estimated for overall data, and category1 for each monsoon season during the period 2006 – 2014. For category 2, only number of the days observed are listed in the Table ST1. As adequate data was not available under category 2 for the correlation analysis, we have obtained the correlation coefficients tropopause and TEJ parameters for all the cases belonging to "far apart" cases as well as "close to each other" cases as listed in the Supplementary Figure ST2. From Tables ST1 and ST2, we observed that our findings for category 1 and category 2 do not change even when all the cases belonging to "close to each other" and "far apart" respectively are taken into consideration. Similar to overall data, no correlation is observed between H_{CPT} and H_{TEJ} for each monsoon season. As the total data in a monsoon season is an amalgam of partly in phase and partly out of phase variations that results in no correlation between H_{CPT} and H_{TEJ} . However, it is interesting to note that H_{CPT} and H_{TEJ} show moderate to strong correlation ($r = 0.43 - 0.78$) significant at 95% confidence level under the category1 during each monsoon season (2006−2014) except 2014. For the year 2014, we have observed four episodes on 23 July –02 August, 7–12 August, 16–19 August and 25–27 August under the category1, in which the first episode shows that H_{CPT} and H_{TEJ} are not in phase as an exceptional case of category1 resulting in an insignificant correlation.

T_{CPT} and H_{TEJ} are significantly anti-correlated ($r = (-0.32) - (-0.40)$) during different monsoon season except 2011 and 2014. T_{CPT} and H_{TEJ} are also significantly anti-correlated ($r = (-0.48) - (-0.79)$) under category1 for each monsoon year except 2011. For each monsoon season, out of phase variation of T_{CPT} and H_{TEJ} are more dominant when compared to their in-phase variation resulting in significant correlation except during the monsoons of 2011 and 2014. Similar to overall data, H_{CPT} and T_{CPT} show weak to moderate ($r = (-0.23) - (-0.63)$) correlation significant at 95% confidence level during different monsoon years. The correlation between H_{CPT} and T_{CPT} under category1 shows moderate to strong anticorrelation ($r = (-0.47) - (-0.83)$) between them for all the monsoon seasons except the monsoon season 2011 suggesting a lack of adiabatic influence in this year. It is to be noted that H_{CPT} and T_{CPT} may not always be driven by adiabatic processes alone and can be affected by other processes such as dynamical heating, ozone heating and occurrence of cirrus clouds (Mehta et al., 2010; Reid & Gage, 1996; Thuburn & Craig, 2000). Thus, when TEJ occurs very close to the CPT and they are strongly correlated it can be considered as an indicator of the prevalence of adiabatic processes. On the other hand, in category2 both H_{CPT} and H_{TEJ} and H_{CPT} and T_{CPT} are poorly correlated which indicates the dominance of the diabatic processes.

Table ST1. *Correlation coefficients between H_{CPT} and H_{TEJ} , T_{CPT} and H_{TEJ} and H_{CPT} and T_{CPT} observed for overall data, category1 and category 2 during the monsoon season 2006–2014. The number of observations is shown under the parentheses. The correlation coefficients shown with an asterisk are significant at 95% confidence level.*

Monsoon Year (JJA)	H_{CPT}×H_{TEJ}			T_{CPT}×H_{TEJ}		H_{CPT} ×T_{CPT}	
	Overall	Category1	Category 2	Overall	Category 1	overall	Category 1
2006	–0.02 (83)	0.72* (50)	14	–0.35*	–0.48*	–0.27*	–0.53*
2007	0.17 (54)	0.78* (27)	6	–0.37*	–0.70*	–0.63*	–0.83*
2008	–0.01 (85)	0.64* (54)	5	–0.32*	–0.46*	–0.23*	–0.47*
2009	0.19 (91)	0.68* (25)	21	–0.36*	–0.64*	–0.42*	–0.72*
2010	0.09 (91)	0.75* (48)	16	–0.35*	–0.61*	–0.26*	–0.55*
2011	0.08 (87)	0.43* (40)	17	–0.13	–0.12	–0.29*	0.10
2012	0.09 (84)	0.56* (45)	3	–0.34*	–0.52*	–0.39*	–0.60*
2013	0.18 (85)	0.70* (35)	17	–0.40*	–0.68*	–0.40*	–0.66*
2014	–0.07 (70)	0.32 (21)	13	–0.18	–0.79*	–0.51*	–0.50*

Table ST2. *Correlation coefficients between H_{CPT} and H_{TEJ} , T_{CPT} and H_{TEJ} and H_{CPT} and T_{CPT} observed for "close to each other" and "far apart" cases during the monsoon season 2006–2014. The number of observations is shown under the parentheses. The correlation coefficients shown with an asterisk are significant at 95% confidence level.*

Monsoon Year (JJA)	H_{CPT}×H_{TEJ}		T_{CPT}×H_{TEJ}		H_{CPT} ×T_{CPT}	
	Close to each other	Far apart	Close to each other	Far apart	Close to each other	Far apart
2006	0.69* (61)	–0.03 (20)	–0.45*	–0.17	–0.60*	0.01
2007	0.71* (40)	–0.04 (14)	–0.61*	0.03	–0.78*	–0.40
2008	0.66* (64)	–0.06 (20)	–0.49*	–0.21	–0.52*	–0.10
2009	0.81* (46)	0.31 (42)	–0.48*	–0.23	–0.59*	–0.27
2010	0.76* (59)	–0.15 (32)	–0.58*	–0.26	–0.47*	–0.12
2011	0.76* (52)	0.18 (39)	–0.38	-0.29	0.32*	–0.26
2012	0.68* (58)	0.08 (25)	–0.57*	–0.39	–0.59*	–0.17
2013	0.73* (53)	0.31 (32)	–0.61*	–0.27	–0.59*	–0.10
2014	0.67* (38)	–0.16 (32)	–0.62*	–0.30	–0.66*	–0.61*

GPS Radiosonde Data

The radiosonde data used in this study is available from dropdown "**view & download data**" listed on the "**Data/Experiment**" tab of the NARL website (www.narl.gov.in)

Steps to download the radiosonde data from NRAL wesite (www.narl.gov.in)

1. Click the tab,"Data/Expreiment"
2. Click on "View & Download data"
3. Click on "GPS radiosonde" tab

Page-1: NARL website main page

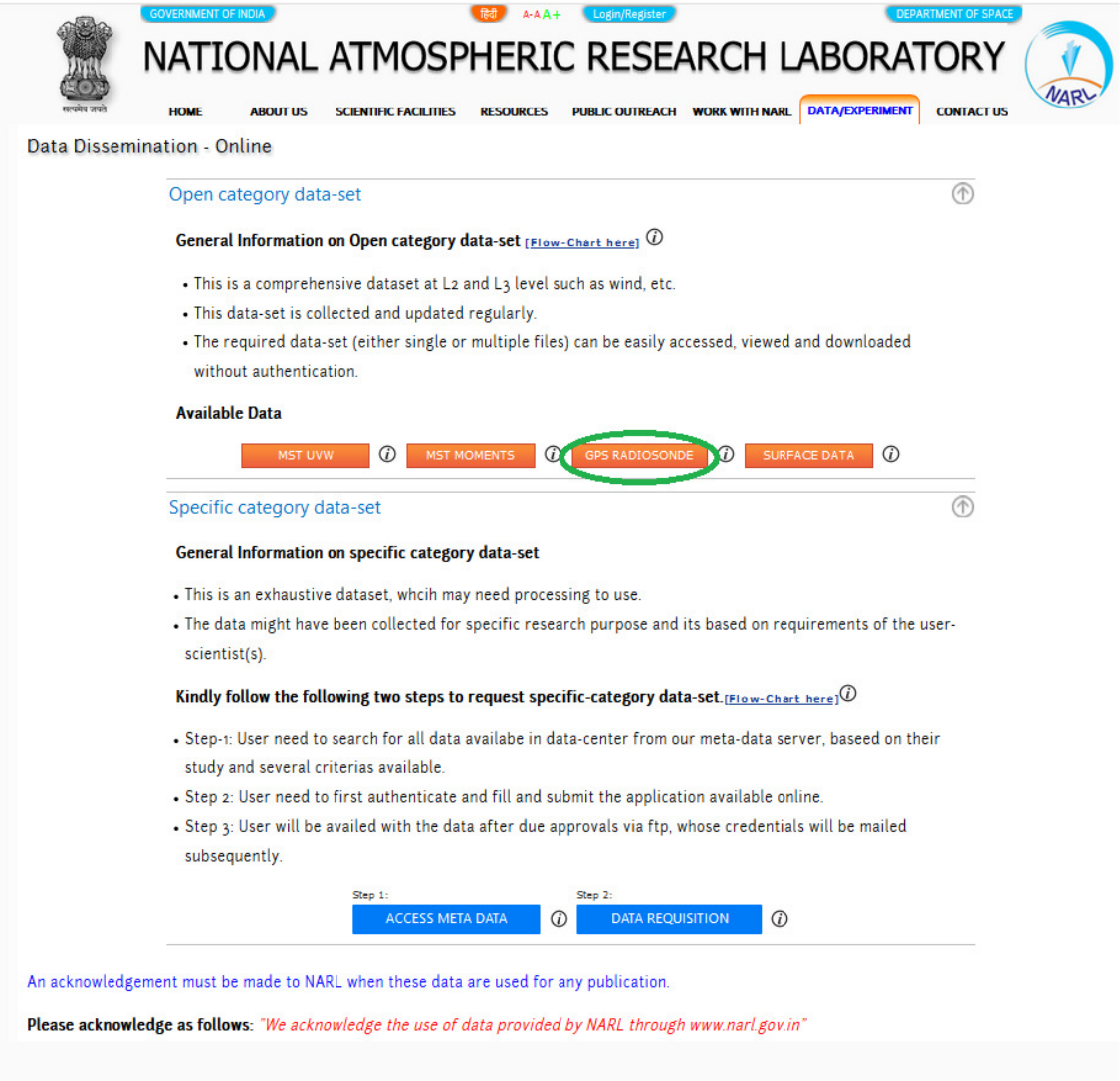

Page-2: Available data page, GPS radiosonde is enricle by green line to download individual date data. One can acess meta data and view the availability of the datasets which can be requested send the link to download it as instrcted.

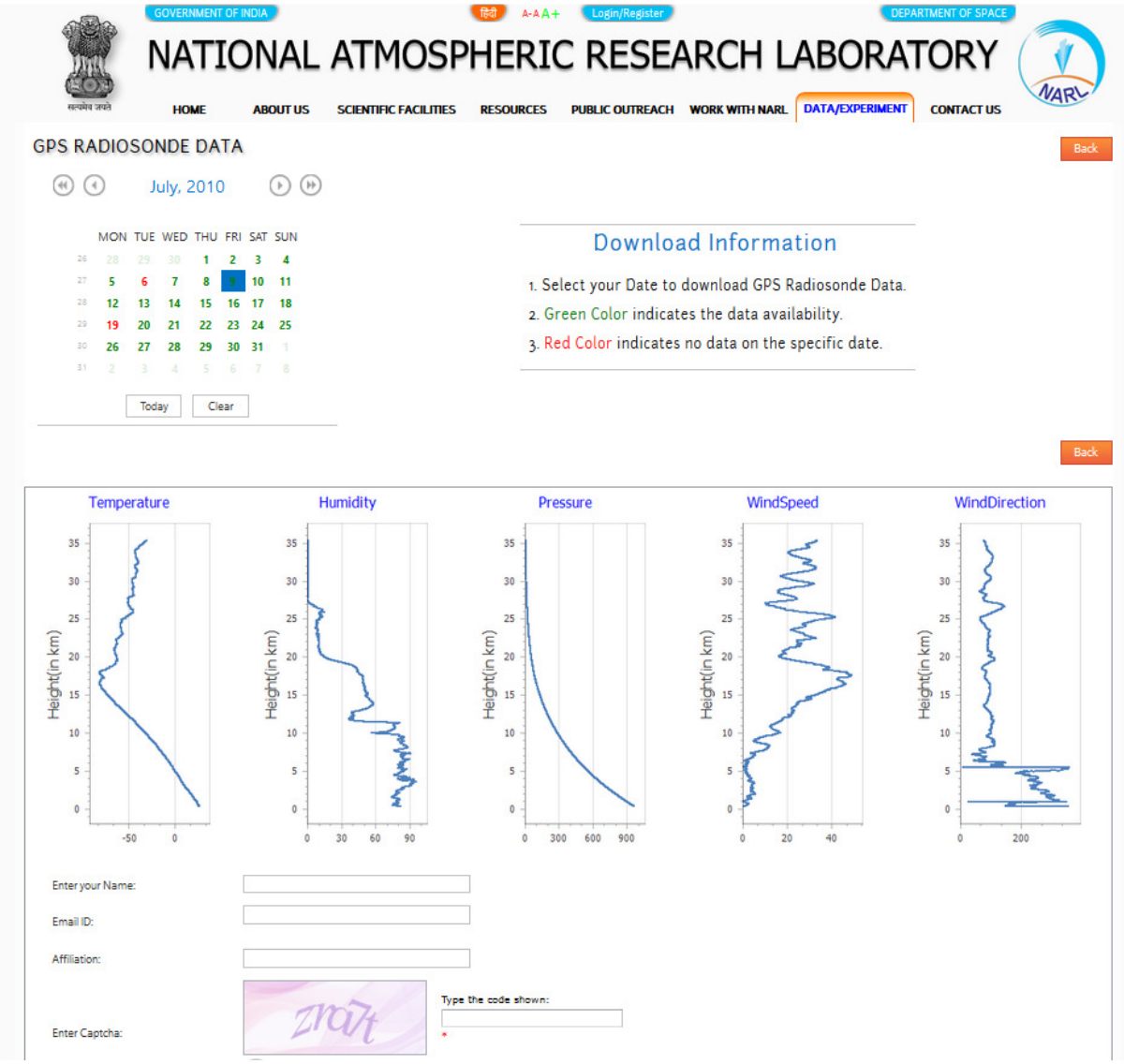

Page-3: Select date and wait for plot to be generated nd fill the required and then dowload. Here typical example is shown for the date 09-07-2010.

References

Highwood, E. J., & Hoskins, B. J. (1998). The tropical tropopause. *Quarterly Journal of the Royal Meteorological Society*, *124*(549), 1579-1604.

Meenu, S., Rajeev, K., Parameswaran, K., Nair, A.K.M., 2010. Regional distribution of deep clouds and cloud top altitudes over the Indian subcontinent and the surrounding oceans. *Journal of Geophysical Research: Atmospheres* 115 (D5).

Mehta, S. K., Venkat Ratnam, M., & Krishna Murthy, B. (2010). Variability of the tropical tropopause over Indian monsoon region. *Journal of Geophysical Research: Atmospheres, 115*(D14).

Reid, G., & Gage, K. (1996). The tropical tropopause over the western Pacific: Wave driving, convection, and the annual cycle. *Journal of Geophysical Research: Atmospheres, 101*(D16), 21233-21241.

Thuburn, J., & Craig, G. C. (2000). Stratospheric influence on tropopause height: The radiative constraint. *Journal of the atmospheric sciences, 57*(1), 17-28.